Rotation of the easy-magnetization direction upon the phase transition from thin iron films to islands on W(110)

1998 J. Phys.: Condens. Matter 10 2873

(http://iopscience.iop.org/0953-8984/10/13/006)

J. Phys.: Condens. Matter **10** (1998) 2873–2880. Printed in the UK PII: S0953-8984(98)87290-1

Rotation of the easy-magnetization direction upon the phase transition from thin iron films to islands on W(110)

L Lu†, J Bansmann and K H Meiwes-Broer

Universität Rostock, Fachbereich Physik, Universitätsplatz 3, D-18051 Rostock, Germany

Received 1 September 1997, in final form 23 December 1997

Abstract. We report on magnetic phenomena exhibited by iron islands on W(110) which have been obtained by evaporating iron at room temperature onto a W(110) surface and finally annealing to about 1000 K. This phase transition from thin films to islands has been studied with LEED and soft-x-ray photoelectron spectroscopy. By virtue of magnetic linear (MLDAD) and circular dichroism (MCDAD) in photoemission, we investigate the magnetic behaviour of both the iron films and the islands. Iron islands exhibit a different easy-magnetization direction as compared to thin iron films.

1. Introduction

Magnetic phenomena exhibited by transition metals in low-dimensional systems have become an attractive subject in recent years. The reduced symmetry and the lower coordination number (number of nearest neighbours) often lead to novel magnetic properties which differ dramatically from those of the respective bulk material, e.g., unexpected magnetic anisotropies or surprisingly low Curie temperatures [1]. Due to the high fundamental and technical relevance of the magnetic nanostructures, a significant theoretical and experimental effort has been devoted to epitaxial thin films and deposited clusters, and has recently brought about considerable progress. Nevertheless, to the best of our knowledge, most of this work has focused on the growth mode, the stability, the electronic properties and the magnetism of thin films. The aim of our paper is to provide experimental information about the magnetic behaviour of iron islands.

In the present article we discuss the magnetic properties of iron islands on W(110), which are created by heating a flat and well-ordered Fe film to temperatures of about 1000 K. The free-surface energies of tungsten and iron result in a layer-by-layer growth mode of iron on this crystal. Also, tungsten is a very convenient substrate as its kinetic barriers are so high that interdiffusion as well as alloy or compound formation are avoided. A detailed experimental analysis of Fe/W(110) has been carried out with, e.g., AES, LEED and TDS [2], spin-resolved photoemission [3, 4], magnetic circular and linear dichroism in UPS [5], STM and STS [6, 7], SPLEED [8], conversion-electron Mössbauer spectroscopy and torsion-oscillation magnetometry (see, e.g., [9]).

The magnetic properties of both the thin iron films and the islands shown in this article have been studied with *magnetic circular and linear dichroism in photoemission* (MCDAD and MLDAD) using tunable synchrotron radiation in the soft-x-ray region. Since magnetic

† Author to whom any correspondence should be addressed; telephone: (+49) 381 498-1670; fax: (+49) 381 498-1667; e-mail: lipinglu@ws1.physik2.uni-rostock.de.

0953-8984/98/132873+08$19.50

dichroism means that the spin-dependent photoexcitation from a ferromagnetically ordered system is already manifested in the photoelectron intensity distributions, MCDAD [10, 11] and MLDAD [12, 13] in photoemission became appropriate techniques for studying magnetic phenomena exhibited by solids and thin films without time-consuming spin resolution. Both experimental methods are theoretically described in several publications [14–16]. Briefly, MCDAD and MLDAD at the spin–orbit-split Fe $3p_{1/2}$ and $3p_{3/2}$ levels arise from an energetic splitting of the m_l-sublevels (m_l: magnetic quantum number), which is induced by the interaction of the core level with the magnetically polarized valence band.

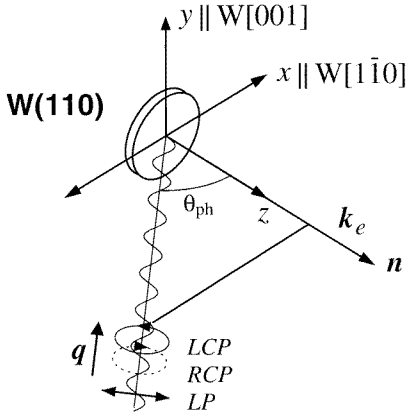

Figure 1. A sketch of the experimental geometry. The W[1$\bar{1}$0] direction is oriented along the x-axis and the W[001] direction along the y-axis. The incoming photon beam lies in the xz-plane, and the angle θ_{ph} is about 60° with respect to the surface normal (the z-axis). The sample is remanently magnetized either along x (in the case of MCDAD) or y (for MLDAD).

2. Experimental details

The experiment was carried out in an UHV chamber (base pressure: 1×10^{-10} mbar) equipped with a four-grid LEED system for surface characterization. Photoelectrons are collected in normal emission using a fixed-in-space electron energy spectrometer with a resolution set to approximately 250 meV. The angle of incidence θ_{ph} is about 60° with respect to the surface normal. As shown in figure 1, the tungsten crystal is oriented with its [1$\bar{1}$0] direction along the x-axis and the W[001] direction parallel to the y-axis. The experimental set-up exhibits a *'chirality'* which is essential for dichroic effects. For MCDAD measurements in normal emission, at least one component of the magnetization vector $\boldsymbol{M}$ has to point along the photon beam direction (in our case, MCDAD: $\boldsymbol{M} \| \boldsymbol{x}$). In contrast, for MLDAD the magnetization has to be perpendicular to the photon beam and to the direction of normal emission (i.e., $\boldsymbol{M} \| \boldsymbol{y}$) to induce a chirality throughout the experimental set-up.

The iron films are prepared at room temperature on a W(110) crystal with an electron beam evaporator using thin rods as the evaporant material. During evaporation the pressure is kept below 4×10^{-10} mbar. An integrated flux monitor facilitates provision of a reproducible growth rate. The tungsten crystal is cleaned by heating in oxygen and flashing to 2600 K. Iron islands are created by heating an epitaxial Fe film to about 1000 K. The magnetization is performed at room temperature by means of a current pulse through two coils close to the sample, either along the x-axis (MCDAD) or the y-axis (MLDAD).

We have carried out these experiments at the storage ring BESSY using the SX700/3 monochromator. The MCDAD technique requires tunable circularly polarized radiation, while for MLDAD linearly polarized light has to be supplied. Storage rings provide linearly (*in-the-orbit-plane*) as well as circularly (*out-of-plane*) polarized radiation over a large photon energy range. The monochromator chosen for our experiments has two separate pre-mirrors for right and left circularly polarized radiation. All of the optical elements are used in grazing incidence to conserve the degree of circular polarization. The degree of circular polarization P_{circ} varies with the photon energy; in this experiment (out-of-plane angle $\psi = \pm 0.9$ mrad, $h\nu = 150$ eV) P_{circ} is about 60% [17].

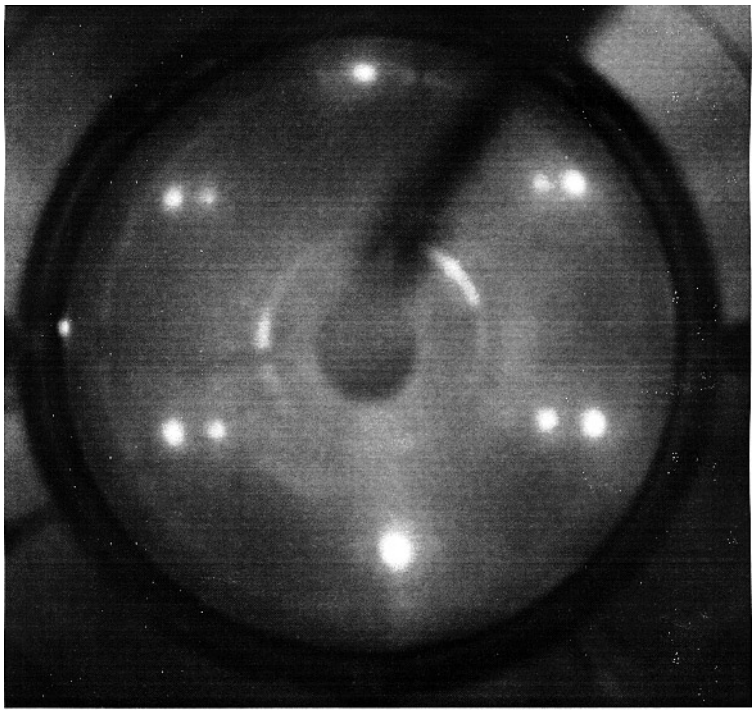

Figure 2. A LEED pattern for iron islands on tungsten. The electron energy of this pattern is 121 eV. The long axis of the reciprocal lattice corresponds to the W[001] direction pointing along the y-axis in figure 1. The inner part is due to the W(110) substrate, while the outer part originates from the bcc (110) iron islands.

3. Results and discussion

The free-surface energies of tungsten and iron ($\gamma_W = 2.9$ J m^{-2}, $\gamma_{Fe} = 2.0$ J m^{-2}) strongly favour monolayer nucleation rather than other possible nucleation modes, such as three-dimensional island formation. Consequently, thermal evaporation of iron on W(110) at room temperature leads to epitaxial bcc (110) Fe films. After the first four layers, which grow as bilayers, are complete, a *Frank–van der Merwe* growth mode (i.e., layer-by-layer growth) is observed. In contrast to the case for bulk iron with its easy-magnetization axis along the $\langle 100 \rangle$ directions, the surface anisotropy causes the easy-magnetization axis for thin Fe films to lie *in the plane* along the $[1\bar{1}0]$ axis [18].

Although there is a large lattice misfit of 9.4%, thermodynamically stable pseudomorphic growth, i.e., with the same lattice parameter as the substrate, is observed up to about two monolayers [2]. Due to the smaller atomic size and lattice constants of iron as compared to those for tungsten, the pseudomorphic monolayers are geometrically strained with respect to the tungsten crystal surface. With the film thickness increasing, the lattice strain plays an even more important role and the periodic lattice distortions compensate for the misfit between the lattice parameter of the bcc W substrate and that of the bcc bulk Fe. The first pseudomorphic monolayer is thermally stable up to 1000 K, whereas multilayers are thermally unstable, either nucleating into 3D islands or evaporating from the substrate above 550 K [2]. No alloy formation has been observed up to now.

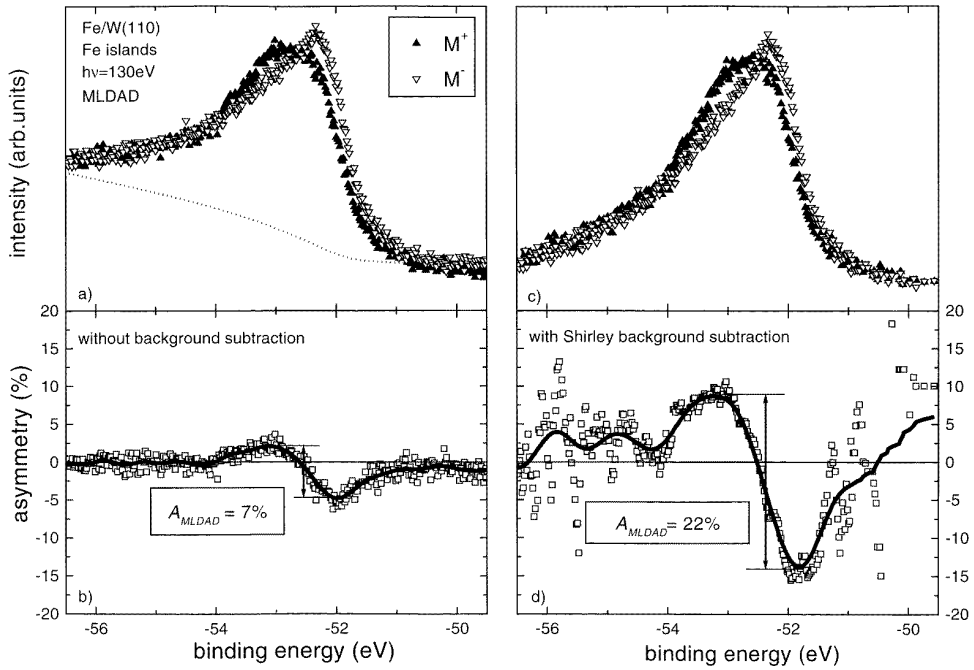

Figure 3. Soft-x-ray photoemission spectra taken for normal emission at 130 eV for opposite magnetization directions (M^+ and M^-). Left-hand panel: the spectrum without background subtraction; the dashed line indicates the Shirley background. Right-hand panel: the same spectrum after background subtraction. The corresponding asymmetries are shown in the lower panels (open squares); the full lines are fitting curves to guide the eye.

The phase transition from the epitaxial films evaporated at room temperature to the island structure is clearly identified by LEED investigation in our experiments (see figure 2). Before heating the iron films (two up to 10 ML Fe), the LEED pattern displays the well-known superstructures published more than ten years ago by Gradmann and co-workers [2]. After heating, we observe LEED patterns of two bcc (110) lattices with different lattice constants at a kinetic energy of 121 eV. The inner part is due to the W(110) substrate, while the outer pattern originates from the bcc (110) Fe islands. A more detailed analysis of the intensity distribution in the LEED spots could give information on the island size distribution [19]. For this purpose, however, a highly resolving system is more appropriate. As a first guess, the island size determined from the spot diameter (FWHM) gives significantly too

small values compared to STM data. In this contribution the LEED records merely serve to monitor the successful phase transition from thin films to an island structure. Recent STM measurements made by our group show that an annealing to about 1000 K does indeed create well-ordered 3D iron islands which are atomically flat on top. Hence, these data confirm previous STM measurements [7] showing that an annealing of iron multilayers on W(110) to about 1000 K causes a nucleation of relaxed bcc (110) Fe islands (with the lattice constant of bulk iron) which are oriented along the W[001] direction. The island height after heating an epitaxially grown 8 ML iron film reaches about 30–50 ML. However, one complete iron layer is still left on the tungsten substrate—cf. data from Mössbauer analysis [9].

Figure 3 shows the Fe 3p energy distribution curves (taken with opposite magnetization directions $\boldsymbol{M}^+$ and $\boldsymbol{M}^-$) and the corresponding asymmetry for iron islands obtained with linearly p-polarized light. The left-hand panel of figure 3 displays a Fe 3p photoemission spectrum without background subtraction. Notice that the peak in figure 3(a) rides on a background of secondary electrons increasing in intensity towards higher binding energy. In order to determine the Fe 3p line-shapes, a Shirley background subtraction (the dashed line in figure 3(a)) has been performed, as shown in the right-hand panel of figure 3. It is worth mentioning here that the asymmetry (i.e. the MLDAD effect) without background subtraction is about 7%, while after background subtraction the asymmetry increases up to 22%, which is approximately a factor of three larger than before (cf. figures 3(b) and 3(d)). It should be noted that there are scatter points in figure 3(d), which correspond to regions of low electron intensity (see figure 3(c)). It is clear that here the intensity difference might be much larger than the corresponding sum, giving rise to the divergence in the corresponding asymmetry function (according to the definition of the asymmetry: $A_{\mathrm{MLDAD}} = (I^+ - I^-)/(I^+ + I^-)$). Without going into a thorough analysis of the energy dependence of the asymmetry, here it is already obvious that the MLDAD effect can lead to extremely high asymmetry values.

For highlighting the different magnetic behaviours of thin iron films and iron islands, now we use both linearly and circularly polarized radiation and magnetize the sample along two directions (i.e., W[1$\bar{1}$0] and W[001]) without rotating it. As examples, we present Fe 3p photoelectron spectra for epitaxial iron films (the left-hand panel in figure 4) and iron islands (the right-hand panel in figure 4) taken with $h\nu = 150$ eV with a film thickness of 6.5 ML. The sample is irradiated with left (LCP) and right circularly polarized (RCP) and linearly p-polarized (LP) light. In order to demonstrate the MLDAD and MCDAD effects simultaneously, we chose a photon energy of 150 eV, for which the two effects are non-vanishing and the two asymmetry values as well as the photon flux from the monochromator are high. The bold curves in the lower part of each panel (with the same scale in figures 4(a)–4(f)) represent fitting curves for the corresponding intensity differences (open squares). When using circularly polarized radiation (the upper four diagrams), the magnetization direction is chosen collinear with W[1$\bar{1}$0] (cf. the inset in figure 4(b)). For linearly polarized (LP) light, on the other hand, the magnetization vector $\boldsymbol{M}$ points along W[001] or Fe[001] (cf. the inset in figure 4(c)). The results for epitaxial iron films (see figures 4(a) and 4(b)) clearly show different photoelectron intensities in the Fe 3p peak maximum, i.e., a magnetic effect, when using circularly polarized radiation with the magnetization $\boldsymbol{M}$ parallel to the W[1$\bar{1}$0] direction. Furthermore, the sign of the intensity difference is reversed by switching the helicity of the incoming photon beam from LCP to RCP or vice versa. Due to the dipole selection rules for circularly polarized light ($\Delta m = \pm 1$), the excited electrons are polarized along the photon spin direction. Reversing the photon helicity leads to an excitation of electrons with opposite spin.

In the case of linearly polarized light (figure 4(c)) with the magnetization vector

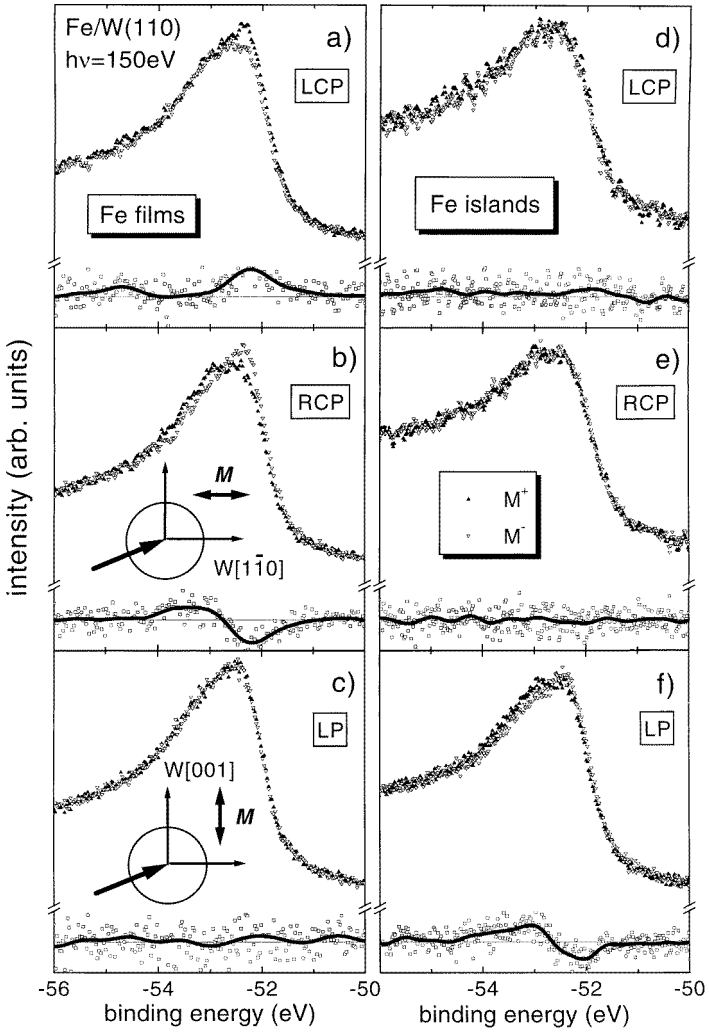

Figure 4. Photoemission spectra from the Fe 3p orbital for iron films and iron islands taken at $h\nu = 150$ eV (for opposite magnetization directions, $\boldsymbol{M}^+$ and $\boldsymbol{M}^-$) with left (LCP) and right circularly polarized (RCP) and linearly p-polarized (LP) light. Lower part of each panel: the corresponding intensity difference (open squares); the bold curves are fitting curves obtained by a simple averaging procedure. The insets represent the magnetization direction: ((a), (b), (d), (e)) $\boldsymbol{M}\|$W[1$\bar{1}$0]; ((c), (f)) $\boldsymbol{M}\|$W[001].

$\boldsymbol{M}\|$W[001], no significant magnetic effect can be observed for Fe films. Obviously, the easy-magnetization direction for thin Fe films always lies *in the plane* along the [1$\bar{1}$0] direction due to the surface anisotropy (cf. figures 4(a)–(c)). One of the interesting results of the present study, shown in the right-hand panel of figure 4, is that the photoemission data for iron islands, on the other hand, display a pronounced MLDAD effect (see figure 4(f)), whereas the MCDAD effect vanishes (cf. figures 4(d)–4(e)). Indeed, these results prove that the island structure can be remanently magnetized in the Fe[001] direction, which is the easy-magnetization axis for bulk iron. Thus the results illustrate a rotation of the easy-

magnetization direction from [1$\bar{1}$0] for thin epitaxial iron films to the [001] axis after creating iron islands on W(110) by heating the thin film to about 1000 K. The effect displayed in figure 4(f) cannot result from a magnetic ordering of the underlying iron monolayer, since the iron thin film has a strong surface anisotropy along the [1$\bar{1}$0] direction. The magnetization direction lying along the [001] axis is favoured by the rectangular shape of the iron islands with the long axis of the Fe rectangle pointing along the W[001] direction; for details of the shapes of the Fe islands, see references [7, 20]. Thus the easy-magnetization axis of thin films along the [1$\bar{1}$0] direction can be understood in terms of a surface anisotropy, whereas for iron islands, the easy-magnetization axis (along the in-plane [001] direction) is induced by the shape anisotropy as well as by the easy-magnetization axis of bulk iron. The size of the iron islands strongly depends on the cleanliness of the substrate and the parameters (temperatures, time) of the subsequent heating. So far it appears as if the island shape and the relaxation in the lattice constant are the dominant factors which determine the rotation of the easy-magnetization axis. The island height, on the other hand, possibly plays a minor role. Nevertheless, this phenomenon is supported by the decreasing influence of the surface anisotropy with increasing thickness of iron. At a coverage of 40–50 ML of epitaxially grown Fe on W(110), the easy-magnetization axis changes from W[1$\bar{1}$0] to the W[001] direction. This effect was first observed by Gradmann and co-workers [18] and later confirmed by different groups [3, 4].

We observe a similar rotation already at a coverage of 2–10 ML and subsequent heating in order to induce island formation. In fact, however, we are not yet able to determine a definite value for the onset of the easy-magnetization rotation, since we started our investigation at a coverage of two monolayers of iron, at which stage this phenomenon was already present. The growth of iron on W(110), especially in the regime from 1 up to 4 ML, exhibits several interesting features. Between 1 and 1.8 ML monolayers, iron evaporated at room temperature forms islands which grow anisotropically along the W[001] direction [6] and, additionally, a perpendicular anisotropy has been observed for films from 1.2–1.5 ML thick [8]. With increasing coverage ($>$1.8 ML), a two-dimensional distortion network appears.

The onset of magnetic effects for Fe/W(110) in the submonolayer regime ($\boldsymbol{M}\|$W[1$\bar{1}$0]) has already been determined together with the coalescence of iron islands (see reference [8]). At the moment, no experimental data are available on the magnetic behaviour ($\boldsymbol{M}\|$W[001]) of iron islands below a corresponding coverage of 2 ML. We will try to extend our experiments into this region.

The magnetic circular and linear dichroism in photoemission are very surface sensitive and enable one to observe magnetic phenomena without spin resolution. On the other hand, it is very difficult to separate the spin and orbital components from the spectra in order to determine the magnetic moments. Possibly, this could be done via model calculations where only one parameter is varied. The first fully relativistic photoemission calculations with respect to MCDAD at the Fe 3p levels are just being carried out [21].

4. Summary

In summary, it should be emphasized that surface anisotropies for thin iron films on W(110) play an important role, giving rise to the easy-magnetization direction lying along the [1$\bar{1}$0] axis. Subsequent heating of the sample leads to the nucleation of incommensurately ordered, flat bcc (110) Fe islands on top of a monolayer of iron on the W(110) crystal. These iron islands are oriented along the W[001] direction and can be magnetized remanently along the easy-magnetization direction of the respective iron bulk crystals, i.e. along the

[001] direction. The influence of the lateral dimensions of the islands and of the thickness distribution has still to be explored. Nevertheless, that there is a rotation of the easy axis upon the phase transition from a thin film to island structure can be clearly stated.

Acknowledgments

We gratefully acknowledge the support by the BESSY GmbH in Berlin and especially the continuous help from Dr W Braun. This work was supported by the Deutsche Forschungsgemeinschaft DFG, the Bundesministerium für Bildung und Forschung BMBF and the European Community.

References

[1] Gradmann U 1993 *Handbook of Magnetic Materials* vol 7, ed K H J Buschow (Amsterdam: North-Holland) pp 1–91
[2] Gradmann U and Waller G 1982 *Surf. Sci.* **116** 539
Berlowitz P J, He J W and Goodman D W 1990 *Surf. Sci.* **231** 315
[3] Kurzawa R, Kämper K P, Schmitt W and Güntherodt G 1986 *Solid State Commun.* **60** 777
[4] Getzlaff M, Bansmann J, Braun J and Schönhense G 1997 *Z. Phys.* B **104** 11
Getzlaff M, Bansmann J, Braun J and Schönhense G 1993 *Solid State Commun.* **87** 467
[5] Bansmann J, Getzlaff M, Ostertag Ch and Schönhense G 1996 *Surf. Sci.* **352–354** 898
Bansmann J 1993 *PhD Thesis* Universität Bielefeld, Germany
[6] Bethge H, Heuer D, Jensen Ch, Reshöft K and Köhler U 1995 *Surf. Sci.* **331–333** 878
Jensen C, Reshöft K and Köhler U 1996 *Appl. Phys.* A **62** 217
[7] Bode M, Pascal R and Wiesendanger R 1997 *J. Vac. Sci. Technol.* A **15** 1285
Bode M 1996 *PhD Thesis* Universität Hamburg, Germany
[8] Elmers H J, Hauschild J, Höche H, Gradmann U, Bethge H, Heuer D and Köhler U 1994 *Phys. Rev. Lett.* **73** 898
Elmers H J, Hauschild J, Höche H, Gradmann U, Bethge H, Heuer D and Köhler U 1995 *Phys. Rev. Lett.* **75** 2031
[9] Przybylski M, Kaufmann I and Gradmann U 1989 *Phys. Rev.* B **40** 8631
[10] Baumgarten L, Schneider C M, Petersen H, Schäfers F and Kirschner J 1990 *Phys. Rev. Lett.* **65** 492
[11] Starke K, Navas E, Arenholz E, Baumgarten L and Kaindl G 1995 *Appl. Phys.* A **60** 179
[12] Roth Ch, Hillebrecht F U, Rose H B and Kisker E 1993 *Phys. Rev. Lett.* **70** 3479
[13] Rossi G, Sirotti F, Cherepkov N A, Combet Farnoux F and Panaccione G 1994 *Solid State Commun.* **90** 557
[14] Venus D 1993 *Phys. Rev.* B **48** 6144
Venus D 1994 *Phys. Rev.* B **49** 8821
[15] Cherepkov N A 1994 *Phys. Rev.* B **50** 13 813
[16] Thole B T and van der Laan G 1991 *Phys. Rev.* B **44** 12 424
Thole B T and van der Laan G 1993 *Phys. Rev.* B **48** 210
Thole B T and van der Laan G 1994 *Phys. Rev.* B **49** 9613
Thole B T and van der Laan G 1995 *Phys. Rev.* B **52** 15 355
[17] Petersen H, Willmann M, Schäfers F and Gudat W 1993 *Nucl. Instrum. Methods Phys. Res.* A **333** 594
Petersen H, Jung C, Hellwig C, Peatman W B and Gudat W 1995 *Rev. Sci. Instrum.* **66** 1
[18] Gradmann U, Korecki J and Waller G 1986 *Appl. Phys.* A **39** 101
[19] Henzler M 1996 *Surf. Sci.* **357+358** 810
Henzler M 1996 *Surf. Sci.* **298** 369
Ertl G and Küppers J 1985 *Low Energy Electrons and Surface Chemistry* (Weinheim: VCH)
[20] Reuter D 1997 *PhD Thesis* Universität Halle-Wittenberg, Germany
Kirschner J 1997 private communication
[21] Braun J 1997 private communication